

Inter-layer Superconducting Pairing Induced c -axis Nodal Lines in Iron-based Superconductors

Yuehua Su,¹ Chandan Setty,² Ziqiang Wang,³ and Jiangping Hu^{2,4,*}

¹*Department of Physics, Yantai University, Yantai 264005, China*

²*Department of Physics, Purdue University, West Lafayette, Indiana 47907, USA*

³*Department of Physics, Boston College, Chestnut Hill, Massachusetts 02467, USA*

⁴*Beijing National Laboratory for Condensed Matter Physics,*

Institute of Physics, Chinese Academy of Sciences, Beijing 100080, China

A layered superconductor with a full pairing energy gap can be driven into a nodal superconducting (SC) state by inter-layer pairing when the SC state becomes more quasi-3D. We propose that this mechanism is responsible for the observed nodal behavior in a class of iron-based SCs. We show that the intra- and inter-layer pairings generally compete and the gap nodes develop on one of the *hole* Fermi surface pockets as they become larger in the iron-pnictides. Our results provide a natural explanation of the c -axis gap modulations and gap nodes observed by angle resolved photoemission spectroscopy. Moreover, we predict that an anti-correlated c -axis gap modulations on the hole and electron pockets should be observable in the S^\pm -wave pairing state.

For the iron-based superconductors [1, 2] with a complicated band structure, the symmetry of the order parameter in the superconducting (SC) state [3] remains elusive. The S^\pm -wave pairing symmetry, predicted by both strong [4–7] and weak coupling theories [8–10] based on the magnetic origin, is a promising candidate and has been supported by many experimental results [6, 11–13]. However, it has also been seriously challenged by the existence of gapless excitations or nodal behavior observed in some iron-based superconductors [14–19], in particular, $BaFe_2As_{2-x}P_x$ [20–23, 25] where some of the As atoms are replaced by the P atoms. A possible explanation of the nodal behavior has been suggested by the weak coupling approaches, such as the functional renormalization group (FRG) technique [27, 28] and random phase approximations (RPA) [26]. These calculations suggest that gap nodes can develop on the electron pockets when the detailed nesting properties vary among the hole pockets located at the Γ and M points, and the electron pockets located at the X point of the unfolded Brillouin zone. When the size of the hole pocket at M point decreases, the SC gap on the electron pockets becomes increasingly anisotropic and eventually gap nodes emerge. The reduction of the M hole pocket can be achieved by either increasing electron doping or by tuning the pnictogen height through replacing As by P [23, 29].

Recently, nodes in the gap function dispersion along in the c -axis (c -axis nodal lines) have been observed directly by ARPES in $BaFe_2As_{1.7}P_{0.3}$ [30]. However, the weak coupling theories cannot explain the observed nodal behavior for the following reasons. First, the observed nodes are on the hole pockets, not on the electron pockets. Second, in contrast to LDA calculations [26], the P substitution in these materials does not push the hole-like band near M to sink below the Fermi surface [21, 25]. Instead, as the substitution increases, the M hole pocket and the X electron pockets barely change while the hole pockets near the Γ point at the zone center ($k_z = 0$),

which have large c -axis dispersions, accommodate the additional holes. As a result, with increasing P substitution, one of the two Γ hole pockets grows increasingly larger. The size of this hole pocket at the Z point ($k_z = \pi$) can even be larger than the size of the largest hole pocket in KFe_2As_2 , the most hole-doped iron-based superconductors known today. These properties point to a non-rigid band picture under the “iso-valent” doping and completely violate the assumption of the band structure taken in the above weak coupling theories.

In this Letter, we suggest that the observed nodal behavior originates from the inter-layer pairing and the reduction of the intra-layer SC pairing gap due to the increase of the size of the hole pockets. This proposal consistently explains the c -axis modulation of the SC gaps observed in optimally hole-doped $Ba_{1-x}K_xFe_2As_2$ [31, 32] and the nodal behaviors in $BaFe_2As_{2-x}P_x$ [30]. It suggests that the gap modulations along the c -axis are directly related to the c -axis band dispersion. Our calculation also reveals that the inter-layer SC pairing, in general, competes with the intra-layer SC pairing in these quasi-two dimensional materials, a possible reason why the highest T_c is not achieved in the 122-family (AFe_2As_2) but in the 1111-family ($AOfeAs$) of the iron pnictides [34, 35] since the former is more three dimensional [2, 33, 37]. Moreover, we predict that the S^\pm -wave pairing symmetry should result in an anti-correlation of the SC gap values between the hole and electron pockets along the c -axis as a function of c -axis momentum. This property, if observed, can serve as a direct experimental evidence for the S^\pm -wave pairing symmetry.

Model We construct a three-orbital model which includes the d_{xz} , d_{yz} and d_{z^2} orbitals to study the physics. Experimentally, the large c -axis dispersion is only observed in one of the hole pockets near the Γ point which is mainly composed of $d_{xz,yz}$ orbitals [36]. The increase of the c -axis dispersion upon P doping is mainly due to the increase of the mixture of the d_{z^2} orbital into this

hole pocket [25]. This has been shown by both polarized ARPES experiments [25] and numerical calculations [29, 38]. The ARPES experiments [25, 30] show that the hole pocket with the large c -axis dispersion has even symmetry with respect to the reflection of the $\Gamma - M$ mirror plane and, with increasing P doping, the band mainly attributed to the d_{z^2} orbital moves closer and closer to the Fermi energy so that the weight of d_{z^2} on the Fermi surface increases. This picture is consistent with the symmetry analysis since the d_{z^2} orbital is also symmetric with respect to the reflection of the $\Gamma - M$ mirror plane. The model we construct captures all the above essential experimental results and can still achieve high analytical tractability. We will also show that the results for the c -axis properties derived from this model are rather generic.

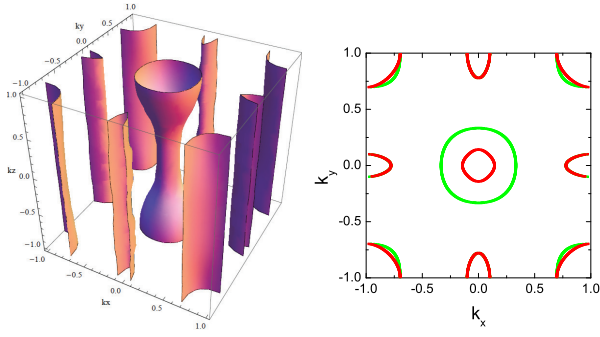


FIG. 1: 3-D Fermi surfaces and Contour plot of Fermi surfaces in the extended three-band model Eq.(1) ($k_z = 0$ for the read line and $k_z = \pi$ for the green line).

The Hamiltonian of our model includes two parts $H = H_t + H_I$, where H_t is the kinetic energy and H_I is the pairing interaction. H_t is given by

$$H_t = \sum_{\mathbf{k}, \alpha\beta\sigma} \varepsilon_{\mathbf{k}\alpha\beta} d_{\mathbf{k}\alpha\sigma}^\dagger d_{\mathbf{k}\beta\sigma}, \quad (1)$$

where $\alpha, \beta = 1, 2, 3$ label the 3d electrons in the d_{xz} , d_{yz} and d_{z^2} orbital respectively. The form of the kinetic energy and the hopping parameters are constructed by extending the two-orbital model [42] to achieve the c -axis dispersion that matches well the experimental results. Their explicit forms are

$$\begin{aligned} \varepsilon_{\mathbf{k},11} &= -2t_1 \cos k_x - 2t_2 \cos k_y - 4t_3 \cos k_x \cos k_y - \mu, \\ \varepsilon_{\mathbf{k},22} &= -2t_2 \cos k_x - 2t_1 \cos k_y - 4t_3 \cos k_x \cos k_y - \mu, \\ \varepsilon_{\mathbf{k},33} &= 2t_z (\cos k_x + \cos k_y) - \mu_3, \\ \varepsilon_{\mathbf{k},12} &= -4t_4 \sin k_x \sin k_y, \\ \varepsilon_{\mathbf{k},13} &= -t_{xz} (1 - \cos k_z) (\cos k_x + \cos k_y) \sin k_x, \\ \varepsilon_{\mathbf{k},23} &= t_{xz} (1 - \cos k_z) (\cos k_x + \cos k_y) \sin k_y. \end{aligned}$$

The c -axis dispersion is induced by the coupling between the $d_{xz,yz}$ and d_{z^2} orbitals. The later is taken to be below the Fermi level. In the explicit form of the coupling

between these orbitals, $\varepsilon_{\mathbf{k},13}$, we have taken into account both the lattice symmetry requirements and the experimental observations. By taking the following parameters $t_1 = -1, t_2 = 1.55, t_3 = t_4 = -0.85, t_z = 1, t_{xz} = 0.8, \mu = 1.77, \mu_3 = 5$, we find that the model describes well the 3-dimensional Fermi surfaces measured experimentally [25, 30] as shown in Fig. 1.

H_I , the SC pairing interaction, generally includes the following terms,

$$\begin{aligned} H_{intra,1} &= -V_1 \sum_{\mathbf{k}\mathbf{k}', \alpha=1,2} \phi_{\mathbf{k}}^{(1)} \phi_{\mathbf{k}'}^{(1)} d_{\mathbf{k}\alpha\uparrow}^\dagger d_{-\mathbf{k}\alpha\downarrow}^\dagger d_{-\mathbf{k}'\alpha\downarrow} d_{\mathbf{k}'\alpha\uparrow} \\ H_{inter,2} &= -V_2 \sum_{\mathbf{k}\mathbf{k}', \alpha=1,2} \phi_{\mathbf{k}}^{(2)} \phi_{\mathbf{k}'}^{(2)} d_{\mathbf{k}\alpha\uparrow}^\dagger d_{-\mathbf{k}\alpha\downarrow}^\dagger d_{-\mathbf{k}'\alpha\downarrow} d_{\mathbf{k}'\alpha\uparrow} \\ H_{inter,3} &= -V_3 \sum_{\mathbf{k}\mathbf{k}'} \phi_{\mathbf{k}}^{(3)} \phi_{\mathbf{k}'}^{(3)} d_{\mathbf{k},3\uparrow}^\dagger d_{-\mathbf{k},3\downarrow}^\dagger d_{-\mathbf{k}',3\downarrow} d_{\mathbf{k}',3\uparrow} \\ H_{inter,4} &= -V_4 \sum_{\mathbf{k}\mathbf{k}'} \phi_{\mathbf{k}}^{(4)} \phi_{\mathbf{k}'}^{(4)} (d_{\mathbf{k},1\uparrow}^\dagger d_{-\mathbf{k},1\downarrow}^\dagger d_{-\mathbf{k}',3\downarrow} d_{\mathbf{k}',3\uparrow} \\ &\quad + d_{\mathbf{k},2\uparrow}^\dagger d_{-\mathbf{k},2\downarrow}^\dagger d_{-\mathbf{k}',3\downarrow} d_{\mathbf{k}',3\uparrow} + h.c.). \end{aligned}$$

The first term $H_{intra,1}$ describes the intra-layer pairing while the rest three terms describe the different inter-layer pairing interactions. $H_{inter,2}$ accounts for the inter-layer pairing interaction between the d_{xz} and d_{yz} orbitals, as does $H_{inter,3}$ for the d_{z^2} orbital. The last term describes the inter-layer interaction between the d_{z^2} and $d_{xz,yz}$ pairs. We take $\phi_{\mathbf{k}}^{(1)}$ to be the intra-layer S^\pm -wave pairing function $\phi_{\mathbf{k}}^{(1)} = \cos k_x \cos k_y$ and $\phi_{\mathbf{k}}^{(2)} = (\cos k_x + \cos k_y) \cos k_z$, and $\phi_{\mathbf{k}}^{(3,4)} = \cos k_z$. These choices rely on the assumption that the SC pairing in iron-based superconductors is rather short-ranged. The form of $\phi^{(1)}$ has been proposed in the models based on local magnetic exchange couplings [4-7] and it has been shown that the form factor is consistent with current experimental results [11]. The form of $\phi^{(2)}$ has been proposed in [32], which can be obtained from the existence of AFM exchange couplings between the layers [39, 40]. The form of $\phi^{(3,4)}$ and the corresponding $V_{3,4}$ pairing interactions can be understood as the inter-layer pairing is between two adjacent layers and the pairing symmetry is s-wave. V_3 describes the inter-layer pairing for the d_{z^2} orbital. The V_4 term, which describes the coupling between two inter-layer pairings of two different orbitals, can be understood in the following way. Since the c -axis hopping term in H_t describes the hopping between two adjacent layers and the d_{z^2} is below the Fermi level, the second order perturbation through such hopping would generically produce $V_4 \propto \frac{t_{xz}^2}{\mu_3}$.

In the self-consistent mean-field theory for the SC state, H_I becomes

$$H_{BCS} = - \sum_{\mathbf{k}\alpha} \Delta_\alpha(\mathbf{k}) d_{\mathbf{k}\alpha\uparrow}^\dagger d_{-\mathbf{k}\alpha\downarrow}^\dagger + h.c., \quad (2)$$

where $\Delta_1(\mathbf{k}) = \Delta_1^{(1)} \phi_{\mathbf{k}}^{(1)} + \Delta_1^{(2)} \phi_{\mathbf{k}}^{(2)} + \Delta_3^{(4)} \phi_{\mathbf{k}}^{(4)}$, $\Delta_2(\mathbf{k}) =$

$\Delta_2^{(1)}\phi_{\mathbf{k}}^{(1)} + \Delta_2^{(2)}\phi_{\mathbf{k}}^{(2)} + \Delta_3^{(4)}\phi_{\mathbf{k}}^{(4)}$ and $\Delta_3(\mathbf{k}) = \Delta_3^{(3)}\phi_{\mathbf{k}}^{(3)} + (\Delta_1^{(4)} + \Delta_2^{(4)})\phi_{\mathbf{k}}^{(4)}$. Here $\Delta_\alpha^{(n)}$ is defined by

$$\Delta_\alpha^{(n)} = V_n \sum_{\mathbf{k}} \phi_{\mathbf{k}}^{(n)} \langle d_{-\mathbf{k}\alpha\downarrow} d_{\mathbf{k}\alpha\uparrow} \rangle. \quad (3)$$

Results Before we present a full numerical solution for the above Hamiltonian, we first discuss the simple physical picture for the generation of the nodal points in the gap function on the hole pocket. In the above model, if we consider the general intra-orbital pairing form of the $d_{xz,yz}$ orbitals, the k_z -dependent SC gap can be written as

$$\Delta(\mathbf{k}) = \Delta_0 [\cos k_x \cos k_y + \delta_z (\lambda + \cos k_x + \cos k_y) \cos k_z], \quad (4)$$

where the first term represents the S^\pm pairing and the second term represents the inter-layer pairing with the S -wave pairing symmetry. In the first order approximation, this intra-orbital pairing roughly determines the SC gap since it dominates as we will show later. This form indicates that the inter-layer pairing is between the two neighboring layers. The gap zero points develop as δ_z increases. As shown in Fig. 2, when δ_z reaches a certain value, the contour of the gap zeroes will cross the Fermi surface at the points near $k_z = \pm\pi$, which leads to the nodal behavior.

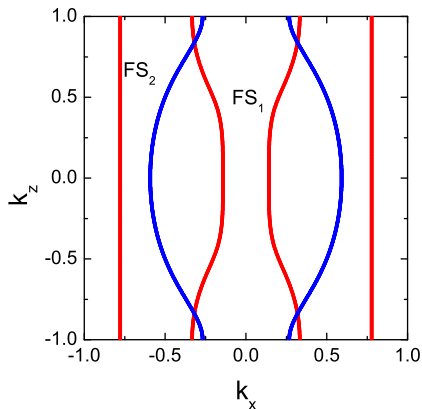


FIG. 2: A cartoon plot for the gap nodal picture in the momentum space $(k_x, 0, k_z)$. The blue lines are the contour lines for zero gap value of Eq. (4) with $\delta_z = 0.4$ and $\lambda = 0$. FS₁ and FS₂ are defined in Fig. 1. The intercept between the blue and the red lines produce the nodes in the hole pocket.

Second, we discuss two important, general results obtained from our model, which are independent of the detailed pairing interaction parameters V_i in H_I . One of these is that the inter-layer pairing always competes with the intra-layer pairing. To demonstrate this more clearly, we switch off V_3 and V_4 and perform a self-consistent solution with V_1 and V_2 . The SC pairing gaps as a function of the interacting parameters are shown in Fig.3. It is very clear that the intra-layer pairing reduces while the

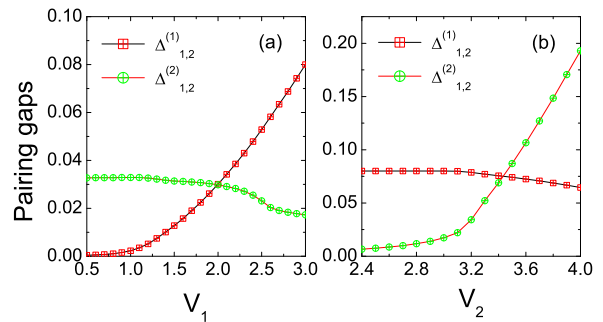


FIG. 3: Gaps versus pairing interactions. Interaction parameters in (a) are defined as $V_2 = 3, V_3 = V_4 = 0$ and (b) $V_1 = 3, V_3 = V_4 = 0$. $\Delta_\alpha^{(n)}$ is defined in Eq. (3).

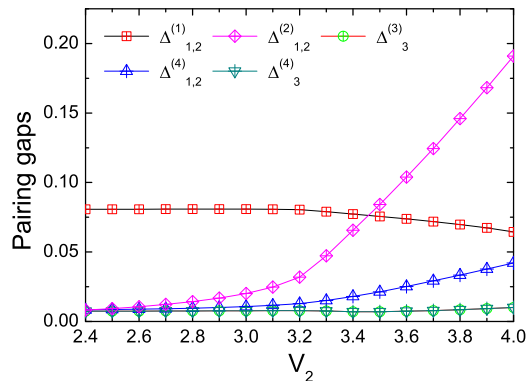


FIG. 4: Gaps versus pairing interaction V_2 with $V_1 = V_3 = V_4 = 3$.

inter-layer pairing increases and vice versa. If we turn on all of the inter-layer pairing interactions, the results are rather similar: while the different inter-layer pairings can increase simultaneously, the intra-layer pairing gaps always decrease as the inter-layer ones increase. A typical result is presented in Fig.4. This result qualitatively suggests that a more quasi two-dimensional SC state is likely better for achieving a higher T_c since the intra-layer pairing would dominate. So far the highest T_c in the iron-based superconductors is achieved in the 1111-family. The highest T_c in the 122 family is about 8 degrees lower than the one in the 1111-family [2]. Comparing to the 122 family, the 1111 family is much more two-dimensional with much less dispersion along the c -axis.

In a multi-orbital model, the relation between the SC pairing parameters and the energy gap in the low energy single particle excitations can be complicated. In order to show that the SC state truly develops nodes, we have to calculate the energy dispersion of the Bogoliubov quasiparticles at the Fermi surfaces. In Fig.5, we plot the dispersion of Bogoliubov quasiparticles along the c -axis with the parameters given by $V_1 = 3, V_2 = 3.35, V_3 = V_4 = 3$. There are two important results. One is that the true

nodes can easily develop on the hole pocket. The other is that the gap values of the quasiparticles on the hole pocket and electron pocket are anti-correlated along the c -axis: the gap value on the hole pocket is larger at $k_z = 0$ than at $k_z = \pi$ while on the electron pocket, it is smaller at $k_z = 0$ than at $k_z = \pi$. This anti-correlation is a combined result of the inter-layer pairing and the S^\pm -wave symmetry for the intra-layer SC pairing order parameter which is proportional to $\cos k_x \cos k_y$ and changes sign between the hole and the electron pocket. This result holds for most of the parameter regions we have investigated. Therefore, this inter-layer pairing induced anti-correlation suggests that ARPES can provide a direct test of the possible S^\pm -wave pairing gap functions in the iron-pnictide superconductors. Of course, to detect it, a high energy-resolution in the ARPES experiments has to be achieved since the c -axis dispersion and the gap modulation on the electron pockets are not large.

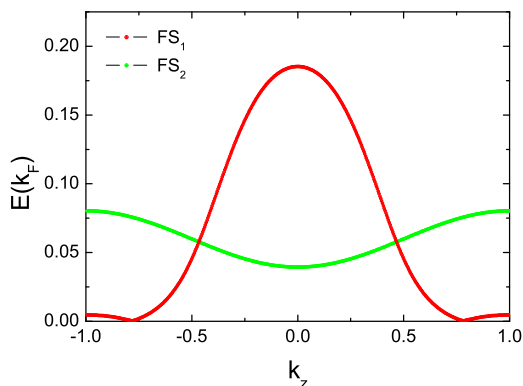


FIG. 5: The energy dispersion of the Bogoliubov quasiparticles at the Fermi surfaces shown in Fig. 1. Here $V_1 = 3, V_2 = 3.35, V_3 = V_4 = 3$ with $\Delta_{1,2}^{(1)} = 0.078, \Delta_{1,2}^{(2)} = 0.057, \Delta_3^{(3)} = 0.007, \Delta_{1,2}^{(4)} = 0.016, \Delta_3^{(4)} = 0.007$.

Finally, we note that several previous thermal conductivity measurements have suggested that the nodes should be on the electron pockets [15]. A key argument given in [15] is that the quasiparticles on the hole pockets have much lower velocity and heavier mass than those on the electron pockets so that the in-plane Fermi velocity V_F of the hole pockets is too small to explain the observed residual thermal conductivity. However, this statement is only partially true. There are three hole pockets centered around the folded Brillouin zone center. The Fermi velocity on one of the hole pockets is in fact comparable to that on the electron pockets. ARPES results [43] show that the former is even slightly larger than the later. This hole pocket, whose orbital character is even with respect to the $\Gamma - M$ mirror plane, is exactly the pocket that carries the large c -axis dispersion. Therefore, the previous thermal conductivity measurements are consistent with our results for the existence of gap nodes on the hole pocket.

Conclusion We have constructed a model to show how nodes in the single-particle excitations can emerge in iron-based superconductors. The development of the nodes are due to the combined effects of the increase in the hole pocket size which reduces the SC gap from intra-layer pairing and the presence of the inter-layer SC pairing. This study consistently explains the experimental observations of the c -axis gap variation in optimally hole-doped $Ba_{1-x}K_xFe_2As_2$ [31, 32] and the nodal behaviors in $BaFe_2As_{2-x}P_x$ [30]. We also demonstrated that the inter-layer and intra-layer pairing generally competes with each other, and suggested a direct experimental test of the S^\pm -wave pairing symmetry through the anti-correlation of the gap modulations on the hole and electron pockets that can be measured by ARPES. We believe that our results can also explain the observed nodal behaviors in other materials such as KFe_2As_2 and $AFe_{2-x}Ru_xAs_2$. A concrete test of our model will be whether the gap functions observed in these materials obey Eq. (4) as the leading contribution to the quasi-3D SC pairing gap function.

Acknowledgement: We thank H. Ding, D. L. Feng, P. C. Dai, N. L. Wang, H. H. Wen and C. Fang for useful discussions. Y.H. is supported by the NSFC (No. 10974167). ZW is supported by DOE DE-FG02-99ER45747.

* Electronic address: hu4@purdue.edu

- [1] Kamihara, Y., Watanabe, T., Hirano, M. & Hosono, H. *J. Am. Chem. Soc.* **130**, 3296, (2008).
- [2] For a review, Johnston D. *Adv. Phys.* **59**, 803, 2010.
- [3] For a review, Hirschfeld, P. J., Korshunov M. M. and Mazin I. I. arXiv:1106.3712 (2011).
- [4] Seo, K., Bernevig B. A., and Hu J., *Phys. Rev. Lett.* **101**, 206404 (2008).
- [5] Fang C., *et al*, *Phys. Rev. X* **1**, (2011).
- [6] Hu, J. and Ding, H. arXiv:1107.1334 (2011)
- [7] Yu R., *et al*. arXiv:1103.3259 (2011).
- [8] Mazin, I. I. *et al*. *Phys. Rev. Lett.* **101**, 057003 (2008).
- [9] Kuroki, K. *et al*. *Phys. Rev. Lett.* **101**, 087004 (2008).
- [10] Wang, F. *et al*. *Phys. Rev. Lett.* **102**, 047005 (2009).
- [11] Ding, H. *et al*. *Europhys. Lett.* **83**, 47001 (2008).
- [12] Zhang Y., *et al*, *Nature Materials* (2010).
- [13] Hanaguri, T. *et al*. *Science*, **328** 474 (2010).
- [14] Hashimoto, K. *et al*. *Phys. Rev. B* **81**, 220501 (2010).
- [15] Yamashita, M. *et al.*, arXiv:1103.0885 (2011).
- [16] Nakai, Y. *et al*. *Phys. Rev. B* **81**, 020503 (2010).
- [17] Cheng B. *et al*. *Phys. Rev. B* **83**, 144522 (2011).
- [18] Zeng B., *et al*, *Nature Communications* **1**, 112 (2010).
- [19] Qiu, X., *et al*, arXiv:1106.5417 (2011).
- [20] Shuai, J. *et al*. *J. Phys.: Condens. Matter* **21**, 382203 (2009).
- [21] Shishido, H. *et al*. *Phys. Rev. Lett.* **104**, 057008 (2010).
- [22] Shuai, J. *et al*. *J. Phys.: Condens. Matter* **21**, 382203 (2009).
- [23] Wang, C. *et al*. *Europhys. Lett.* **86** 47002 (2009).
- [24] Zhang, Y. *et al*. arXiv:1109.0229 (2011).

- [25] Ye Z.R. *et al.* arXiv:1105.5242 (2011).
- [26] Kuroki, K., *et al.* *Phys. Rev. B* **79**, 224511 (2009).
- [27] Wang, F., Zhai, H. & Lee, D.-H. *Phys. Rev. B* **81**, 184512 (2010).
- [28] Thomale, R., *et al.* *Phys. Rev. Lett.* **106**, 187003 (2011).
- [29] Suzuki, K., Usui, H. & Kuroki, K. *J. Phys. Soc. Jpn.* **80** (2011).
- [30] Zhang, Y. *et al.* arXiv:1109.0229 (2011).
- [31] Zhang, Y. *et al.* *Phys. Rev. Lett.* **105**, 117003 (2010).
- [32] Xu, Y.M., *et al.* *Nature Physics*, **7**, 198 (2011).
- [33] Yuan, H. Q. *et al.* *Nature*, **457**, 565 (2009).
- [34] Ren Z. *et al.*, *Chin. Phys. Lett* **25**, 2215 (2008).
- [35] Chen X.H. *et al.*, *Nature* **453**, 761 (2008).
- [36] Zhang Y. *et al.*, *Phys. Rev. B* **83**, 054510 (2011).
- [37] Chi S. *et al.*, *Phys. Rev. Lett* **102**, 107006 (2009).
- [38] Wang G. *et al.*, *Phys. Rev. Lett* **104**, 047002 (2010).
- [39] Zhao J. *et al.*, *Nature Physics* **5**, 555 (2009).
- [40] Zhao J. *et al.*, *Phys. Rev. Lett.* **101**, 167203 (2008).
- [41] Zhang Y. *et al.*, *Phys. Rev. B* **83**, 054510 (2011).
- [42] Raghu S. *et al.*, *Phys. Rev. B* **77**, 220503 (2008).
- [43] Ding H. *et al.*, *J. Phys. Cond. Matt.* **23**, 135701 (2011).